Thin–Walled Structures 205 (2024) 112356

Contents lists available at ScienceDirect

Thin-Walled Structures

journal homepage: www.elsevier.com/locate/tws

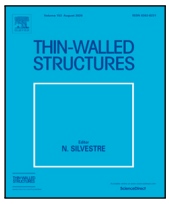

Full length article

Pure distortion of symmetric box beams with hinged walls

Carlos Lázaro [a,*], Guillermo Martínez-López [b,c], Kai-Uwe Bletzinger [b], Roland Wüchner [d]

[a] Dept. de Mecánica de los Medios Continuos y Teoría de Estructuras, Universitat Politècnica de València, Camino de Vera, s/n, Valencia, 46022, Spain
[b] Lehrstuhl für Statik, Technische Universität München, Arcisstr. 21, München, 80333, Germany
[c] Universitat Politècnica de València, Camino de Vera, s/n, Valencia, 46022, Spain
[d] Institut für Statik und Dynamik, Technische Universität Braunschweig, Universitätsplatz 2, Braunschweig, 38106, Germany

ARTICLE INFO

Keywords:
Distortion
Distortional moment
Warping
Torsion
Box girders
Beam theory
Hinged walls

ABSTRACT

This paper is concerned with the analysis of the pure torsion and distortion of straight box beams with trapezial cross-sections and hinged walls. A one-dimensional mechanical model for this kind of system subjected to anti-symmetric loads on the end cross-sections and no warping constraints is developed. The distortional stiffness of the system is provided by the torsional rigidity of the wall panels. The cross-sectional kinematic condition for which torsion and distortion are uncoupled has been determined. Novel explicit expressions of the internal and external distortional moments, the distortion constant, and the distortional warping pattern have been deduced; they can be directly translated to the classical distortion theory. Results of representative test cases with different section shapes and loads show excellent agreement with finite element models using shell elements. The model is a first step to analyse bridge decks with a distortionable central cell for wind engineering applications. Finally, an extension of the model, including the distortional stiffness provided by the frame bending stiffness of the cross-section walls, is presented. The extended model is applicable to assess the large-scale torsional–distortional effects in long beams with closed cross sections.

1. Introduction

Bridge deck girders are generally designed to avoid any significant in-plane deformation of their cross-sections. This kind of deformation is called distortion. In a typical bridge box girder, distortion is controlled by means of diaphragms (in concrete bridges) or stiffening frames/trusses (in steel and composite bridges) located at convenient distances inside the box beam. An adequate control of the distortion ensures the beam-like behaviour of girders whose cross-section proportions are sometimes far from the typical proportions of a structural beam cross-section.

The original motivation of this paper is the search of a novel strategy to mitigate wind-induced vibrations of long-span bridges. The authors have proposed a novel approach consisting of bridge decks composed of two symmetric box girders joined by a deformable central cell [1]. The central cell is allowed to distort in a controlled manner, adding a non-conventional degree of freedom to the deck, when considered as a beam-like structural element (Fig. 1). By adequately tuning the distortional and the torsional natural frequencies of the deck, a significant increase in the critical flutter velocity can be achieved. Testing this strategy, either in a wind tunnel facility or through numerical simulations, requires an efficient one-dimensional (1D) model to evaluate the mechanical properties and the vibrational response of the non-conventional distortion-controlled girder. Before addressing this ultimate goal, which remains out of the scope of this article, this research deals with the problem of the distortional behaviour of symmetric box-girder-like assemblies with trapezial shape and hinged walls, resembling the central cell of the cross-section depicted in Fig. 1.

There is an extensive body of knowledge on the mechanics of distortion of box girders. Vlassov [2] pioneered the study of distortion by modelling the behaviour of a closed rectangular box cross-section by means of a linear combination of assumed deformation patterns — one of which corresponded to the torsional and distortional warping,— whose coefficients were the unknown functions to be determined. Wright et al. [3] developed the analysis of distortion of box girders using the analogy to the deflection of a beam on elastic foundation. The theory was further developed and completed for curved beams by Dabrowski [4], and for tapered beams by Křístek [5]. Steinle [6] summarised the theory and assessed the importance of the assumption of neglecting the shear deformation of the section walls. Boswell and Zhang formulated a curved box beam finite element that considered distortion [7], analysed the distribution of anti-symmetric external forces as shear-flow resultants along the walls and the definition of distortional moment [8], and studied the relation between torsional and distortional warping patterns [8,9] (Boswell and Li).

* Corresponding author.
E-mail address: carlafer@mes.upv.es (C. Lázaro).

https://doi.org/10.1016/j.tws.2024.112356
Received 18 March 2024; Received in revised form 30 July 2024; Accepted 17 August 2024
Available online 22 August 2024

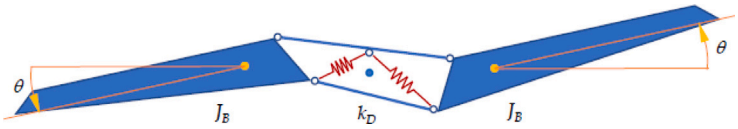

Fig. 1. Distortion-controlled deck cross-section.

The classical approach to the analysis of distortion of box cross-sections is based on the fact that the distortion between stiffening frames is resisted by in-plane bending deformation of the individual wall plates. The derivative of the distortional warping pattern is assumed to be equal to the piecewise constant distribution of tangential displacements in distortion. In closed cross-sections, this assumption is equivalent to neglecting the average in-plane shear strain in the cross-section plates (cf. [8]). It is the same assumption made in the analysis of restrained torsional warping in open cross-sections, but it contradicts the case of pure torsion of box cross-sections. The latter requires adding a shear flow around the cells, causing the in-plane shear deformation that ensures warping compatibility along the cross-section midline [9]. However, the assumption has been commonly adopted to formulate box beam finite elements including distortional modes, e.g. Kim and Kim [10] (for single-cell rectangular box beams in the static case), Park et al. [11] (for multiple-cell rectangular box beams), or recently Zhao et al. [12] and Campo-Rumoroso et al. [13].

More refined torsion–distortion theories that consider in-plane shear flow for warping compatibility are based on Schardt's Generalised Beam Theory (GBT) [14] that systematises and expands Vlassov's [2] and Benscoter's [15] concept of cross-section deformation modes for closed cross-sections. (See Camotim et al. [16] for an overview of GBT.) Following the systematic of deformation modes, Jönsson [17] developed a general orthogonalisation method to determine the warping functions associated with different deformation modes of open and closed cross-sections and noted that uncoupling distortion and torsion in closed cross-sections is in general not possible because of the required compatibility of induced shear flows [18]. Kim and Kim [10] followed a similar approach for general shaped cross-sections. Based on these concepts, Andreassen and Jönsson developed a thin-walled beam element including the distortion of the cross-section [19], and recently Cambronero-Barrientos et al. [20] proposed a similar element including shear lag. More complex cross-section deformation modes can be evaluated by refining the discretisation of the cross section, as e.g. Gonçalves et al. [21], but the selection of representative modes becomes challenging. The requirement of a shear flow to ensure warping compatibility in the deformation of the closed cross-section is crucial in our subsequent developments.

While the presented state-of-the-art includes beam finite elements that can simulate box beams considering torsion and distortion, there are conceptual questions related to the phenomenon of distortion that still deserve careful consideration. We address them in this paper: firstly, the relation between cross-section warping and the coupling between torsion and distortion; secondly, the evaluation of consistent distortional moments that are usually defined using simplifying equilibrium arguments not applicable to general loading patterns (e.g. [8,11] for multi-cell cross-sections).

This paper aims to develop a theory of *pure* distortion of beams with box cross-section and one axis of symmetry, analogous to the theory of pure torsion. For that purpose, anti-symmetric forces are assumed to act only at the end cross-sections, and wall panels are allowed to deform with no external warping constraints. There are two mechanisms to resist distortional loads: The first is the intrinsic resistance provided by the torsional stiffness of the individual walls; it can be analysed by considering the beam as an assembly of hinged walls. The second mechanism is the additional stiffness against distortion provided by out-of-plane bending of the walls or by other devices such as diaphragms or springs (Fig. 2). The bulk of our paper is

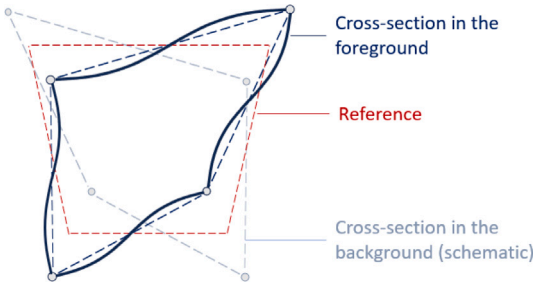

Fig. 2. Resisting mechanisms in pure distortion: torsional stiffness of the walls of a hinged assembly (dashed-blue); out-of-plane bending stiffness of the walls as frame (dark blue).

focused on studying of the hinged assembly, which becomes essential for the consistent formulation of the model. The development starts with analysing the kinematics and evaluating the shear flow needed for compatibility, following [17]; then, the virtual work principle is applied to derive consistent internal forces and external loads. The main results are: (1.) The explicit definition of the distortional warping pattern for symmetric trapezial cross-sections that includes a shear-flow induced term similar to the one present in the torsional warping pattern of box cross-sections; (2.) The constitutive definition of the internal torsional and distortional moment, including the explicit definition of the section constants that relate them to the torsional and distortional strains; (3.) The kinematic condition that uncouples torsion and distortion; (4.) The consistent definition of the external distortional moment from any anti-symmetric set of external point or surface forces. The distortional stiffness provided by the frame bending of the wall plates is considered in the last part of the paper; the corresponding term is included in the virtual work principle to provide a complete formulation of the theory of pure torsion and distortion of box beams with one axis of symmetry. Additionally, with this model, we lay the foundation to analyse the behaviour of composite cross-sections with distortionable core — as in Fig. 1 —, as stated at the beginning of the introduction.

We follow a progressive approach to the problem: Section 2 introduces the simple problem of a box beam with a square cross-section and hinged walls; Section 3 analyses the pure distortion of a doubly symmetric rectangular cross-section; in Section 4, the analysis will be extended to the uniform torsional and distortional behaviour of symmetric trapezial cross-sections when anti-symmetric forces act on the corners of both end sections; finally, Section 5 completes the model by adding a distributed distortional stiffness term and presents, as an extension, a simplified theory for variable torsional and distortional moment densities acting along the beam; Section 6 summarises the conclusions.

In all subsequent developments, we assume linear elastic material, small strains and small displacements (first-order theory). The following assumptions hold for the beam: (1.) Walls are made of thin or moderately thin plates compared to the width of each plate; (2.) The beam is sufficiently constrained in the mid-cross-section to avoid global rigid body motions; (3.) The warping component (parallel to the beam centreline) of the displacement of each material point is not constrained and is constant along every line parallel to the beam centreline; (4.) Self-weight is neglected.

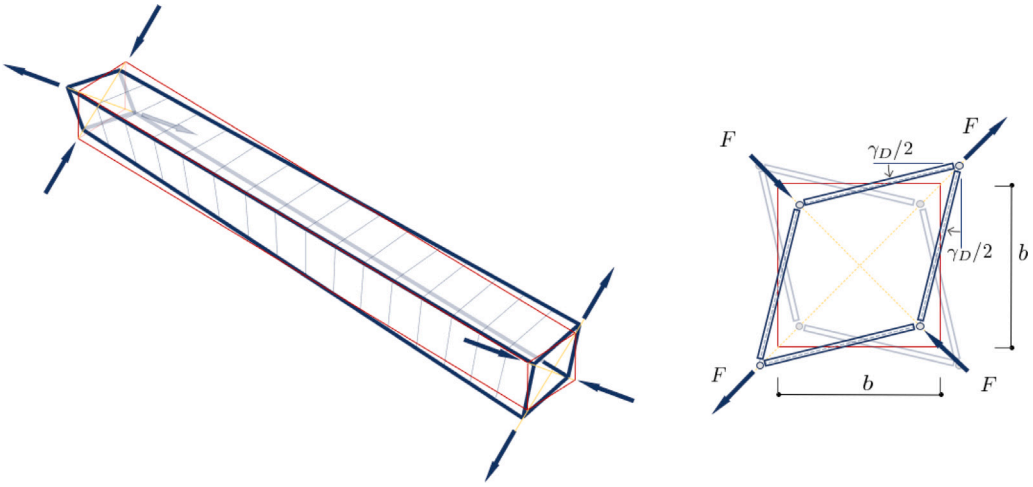

Fig. 3. Left: distortion of a square box assembly with hinged walls: initial shape (red) and distorted shape (blue). Right: kinematics of end cross-sections (background cross-section in dimmed colour).

2. Pure distortion of a square box beam

The simplest example of the intrinsic distortional stiffness provided by the torsional rigidity of the individual walls is given by a box beam with continuously hinged corners and square cross-section of side b in which all walls have the same thickness t (Fig. 3). Assuming that rigid body motions of the full beam are restrained, forces are applied on every corner of the end sections; their orientation is such that triggers the distortion of cross-sections. Note that at each end section, the applied forces are oriented along the diagonals of the section, they cancel out along each diagonal, and they are opposed to the forces acting on the other diagonal. Because of the double symmetry of the cross-section, the displacements of each corner are directed along the diagonals as well. The rate of torsional rotation of the top and bottom plates (flanges) is equal to $\gamma_D'/2$ (constant), where $\gamma_D(x)$ is the distortion angle (change of the angle formed by adjacent walls), and the rate of torsional rotation of the lateral plates (webs) is equal to $-\gamma_D'/2$. If the diagonal forces are decomposed in the horizontal and vertical direction, and their components are assumed to act perpendicularly on the corresponding plate, it is clear that each plate is subjected to a constant torque of magnitude $Fb/\sqrt{2}$. This torque will cause each plate to twist with the following constant rate of rotation:

$$\theta' = \frac{Fb}{\sqrt{2}GJ_w}, \tag{1}$$

where the torsion constant of each thin wall plate is $J_w = \frac{1}{3}bt^3$. As this rate of rotation is equal to $\gamma_D'/2$, the following constitutive relation between external load and rate of distortion follows:

$$2\,\frac{Fb}{\sqrt{2}} = GJ_w\,\gamma_D'. \tag{2}$$

A way to interpret this expression is that the sum of the magnitudes of the torsional moments acting on one flange and on one web cause the rate of distortion of the cross-section given by the formula. We can think of $2Fb/\sqrt{2}$ as a generalised distortional moment, and J_w being the distortion constant. This simple example shows that the hinged assembly of plates possesses an intrinsic stiffness to resist a pure distortional load.

If the walls are thin, the stiffness of the assembly will be very low. In the limit, when the torsional stiffness of the plates is neglected, the hinged assembly is a mechanism. The distortional stiffness can be, of course, increased by adding diaphragms or stiffening frames. In this case, the contribution of the torsional stiffness of the individual plates may become negligible compared to the contribution of the frames. (This is the situation when considering the distortion of bridge box girders.)

The analysis of sections different from the doubly symmetric square one becomes more involved because an additional shear flow is needed to enforce the compatibility of the warping pattern.

3. Pure distortion of doubly-symmetric rectangular box beams

In this section, the pure distortional behaviour of doubly symmetric rectangular box beams with hinged walls is analysed.

3.1. Kinematics

Assuming that the beam is only subjected to a pure distortional set of loads with zero force and moment resultants, the distorted shape of a doubly-symmetric rectangular cross-section must have the following properties:

- Anti-symmetry.
- The rotation centres of the flanges are located on the vertical symmetry axis of the cross-section.
- The rotation centres of the webs are located on the horizontal symmetry axis.
- Pairs of adjacent rotation centres are located on the straight line passing through the corresponding corner of the cross-section.

These conditions are reflected in Fig. 4; note that the position of the rotation centres is fully determined by a single parameter. Selecting D (horizontal distance from the centres of rotation of the webs to the vertical symmetry axis) as independent parameter, the distance d_f is given by the following relation:

$$\frac{d_f}{b/2} = \frac{d_f + h/2}{D} \qquad \Rightarrow \qquad d_f = \frac{bh}{2(2D-b)}. \tag{3}$$

In this section, the kinematics of the cross section is referred to coordinate systems adapted to the walls of the cross-section and centred in each wall (Fig. 4): s is the arc-length coordinate, with origin on the mid-point of the wall mid-line, positive when advancing counter-clockwise, and η is the transverse coordinate, positive when pointing inwards.

The in-plane displacements of the centreline are functions of the rotations of each wall: $\theta_f(x)$ for the flanges, and $\theta_w(x)$ for the webs. As the motion is considered to be infinitesimal, the distortional displacements at a given point of the mid-line can be obtained as the product of the

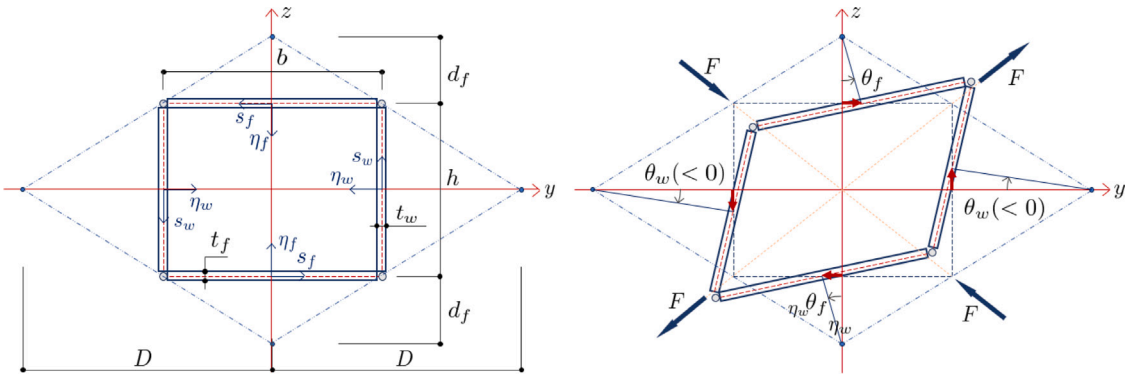

Fig. 4. Parameters and reference systems (left), and distortional deformation mode (right).

distance to the centre of rotation times the rotation angle of each panel:

Flange: $$u_{s,f}(x, s_f) = u_{s,f}(x) = -d_f\,\theta_f(x), \tag{4a}$$

$$u_{\eta,f}(x, s_f) = s_f\,\theta_f(x). \tag{4b}$$

Web: $$u_{s,w}(x, s_w) = u_{s,w}(x) = -(D - b/2)\,\theta_w(x), \tag{4c}$$

$$u_{\eta,w}(x, s_w) = s_w\,\theta_w(x). \tag{4d}$$

Note that the displacements in the centreline direction do not depend on the arclength coordinate (s_f or s_w) and are constant along each wall.

The displacement of every corner must be the same when calculated on the flange and on the web. Selecting, for example, the horizontal component of the upper right corner yields:

$$-d_f\,\theta_f(x) = (h/2)\,\theta_w(x). \tag{5}$$

Therefore, from (3), the following relation between angles holds:

$$\frac{b}{2D - b}\theta_f(x) = -\theta_w(x). \tag{6}$$

The distortion angle $\gamma_D(x)$ is defined as the average of the change in the angle of opposite corners of the cross-section. The change in each opposite corner is the difference of the signed rotations of the adjacent flange and web. Hence,

$$\gamma_D(x) = \theta_f(x) - \theta_w(x). \tag{7}$$

Signed angles (positive ≡ counterclockwise) are used in the formula. By joining Eqs. (6) and (7), the following relations between the rotation angles of the walls and the distortion yield:

Flange: $$\theta_f = \left(1 - \frac{b}{2D}\right)\gamma_D(x), \tag{8a}$$

Web: $$\theta_w = -\frac{b}{2D}\,\gamma_D(x). \tag{8b}$$

Substituting these into Eqs. (4), the displacements of the mid-line in the arc-length and in the normal directions are expressed in terms of the arc length and of the x coordinate:

Flange: $$u_{s,f}(x, s_f) = u_{s,f}(x) = -\frac{bh}{4D}\,\gamma_D(x), \tag{9a}$$

$$u_{\eta,f}(x, s_f) = \left(1 - \frac{b}{2D}\right)s_f\,\gamma_D(x). \tag{9b}$$

Web: $$u_{s,w}(x, s_w) = u_{s,w}(x) = \left(1 - \frac{b}{2D}\right)\frac{b}{2}\,\gamma_D(x), \tag{9c}$$

$$u_{\eta,w}(x, s_w) = -\frac{b}{2D}s_w\,\gamma_D(x). \tag{9d}$$

Fig. 5 shows the rigid-body part of the warping displacements in the longitudinal direction x induced by the distortion. The displacement $u_{s,f}$ causes the flange to rotate along the vertical symmetry axis of the mid cross-section. The value of this rotation is — see (9) —

$$\frac{u_{s,f}|_{x=0.5L}}{0.5L} = -\frac{bh}{4D}\,\gamma'_D, \tag{10}$$

where $\gamma'_D = \gamma_D|_{x=0.5L}/(0.5L)$ denotes the (constant) rate of distortion. Similarly, the displacement $u_{s,w}$ causes the web to rotate along the horizontal symmetry axes of the mid cross-section, and the value of this rotation is

$$\frac{u_{s,w}|_{x=0.5L}}{0.5L} = \left(1 - \frac{b}{2D}\right)\frac{b}{2}\,\gamma'_D. \tag{11}$$

Therefore, the warping displacements caused by these rigid body rotations of the flange and web walls are:

Flange: $$u^{\text{rbm}}_{x,f}(s_f)|_{x=0.5L} = -s_f\,\frac{u_{s,f}|_{x=0.5L}}{0.5L} = \frac{h}{2}\,\frac{b}{2D}\,s_f\,\gamma'_D. \tag{12a}$$

Web: $$u^{\text{rbm}}_{x,w}(s_w)|_{x=0.5L} = -s_w\,\frac{u_{s,w}|_{x=0.5L}}{0.5L} = -\frac{b}{2}\left(1 - \frac{b}{2D}\right)s_w\,\gamma'_D. \tag{12b}$$

Signs are consistent with the orientation of the displacements. Note that, at every corner, the warping of the flange and the warping of the web are incompatible, *unless* the choice $D = b$ is made.

The twisting moment resisted by each wall of the cross-section is:

Flange: $$M_{x,f} = GJ_f\theta'_f = \left(1 - \frac{b}{2D}\right)GJ_f\,\gamma'_D. \tag{13a}$$

Web: $$M_{x,w} = GJ_w\theta'_w = -\frac{b}{2D}GJ_w\,\gamma'_D, \tag{13b}$$

where J_f, J_w are the torsion constants of the flange and of the web. The initial assumption is that the beam is only subjected to distortional loads with zero force and moment resultants. As, in general, $M_{x,f}$ and $M_{x,w}$ will not cancel out, it follows that the section walls must be subjected to a shear flow such that (a) warping due the rigid-body motion plus the shearing of the walls is compatible, and (b) the total moment resultant on the cross section is null.

To enforce warping compatibility, a constant shear N_{xs} must flow along the cross section (positive if counter-clockwise). Using the centres of the walls as origin, the warping due to the shear deformation is:

Flange: $$u^{\text{shear}}_{x,f}(x, s_f) = s_f\,\frac{N_{xs}}{Gt_f}. \tag{14a}$$

Web: $$u^{\text{shear}}_{x,w}(x, s_w) = s_w\,\frac{N_{xs}}{Gt_w}. \tag{14b}$$

Enforcing warping compatibility at the corners,

$$\left(u^{\text{rbm}}_{x,f} + u^{\text{shear}}_{x,f}\right)|_{s_f=-\frac{b}{2}} = \left(u^{\text{rbm}}_{x,w} + u^{\text{shear}}_{x,w}\right)|_{s_w=+\frac{h}{2}}, \tag{15}$$

yields

$$N_{xs} = G\left(1 - \frac{b}{D}\right)\frac{bh}{\frac{2b}{t_f} + \frac{2h}{t_w}}\,\gamma'_D. \tag{16}$$

This shear flow is statically equivalent to the following torsional moment:

$$M^{\text{shear}}_x = 2bh\,N_{xs} = G\hat{J}\,\frac{1}{2}\left(1 - \frac{b}{D}\right)\gamma'_D, \tag{17}$$

where $\hat{J} = 4(bh)^2/(2b/t_f + 2h/t_w)$ is the torsion constant of the box cross-section resulting from Bredt's formula, i.e. assuming that the thickness of the walls is very small.

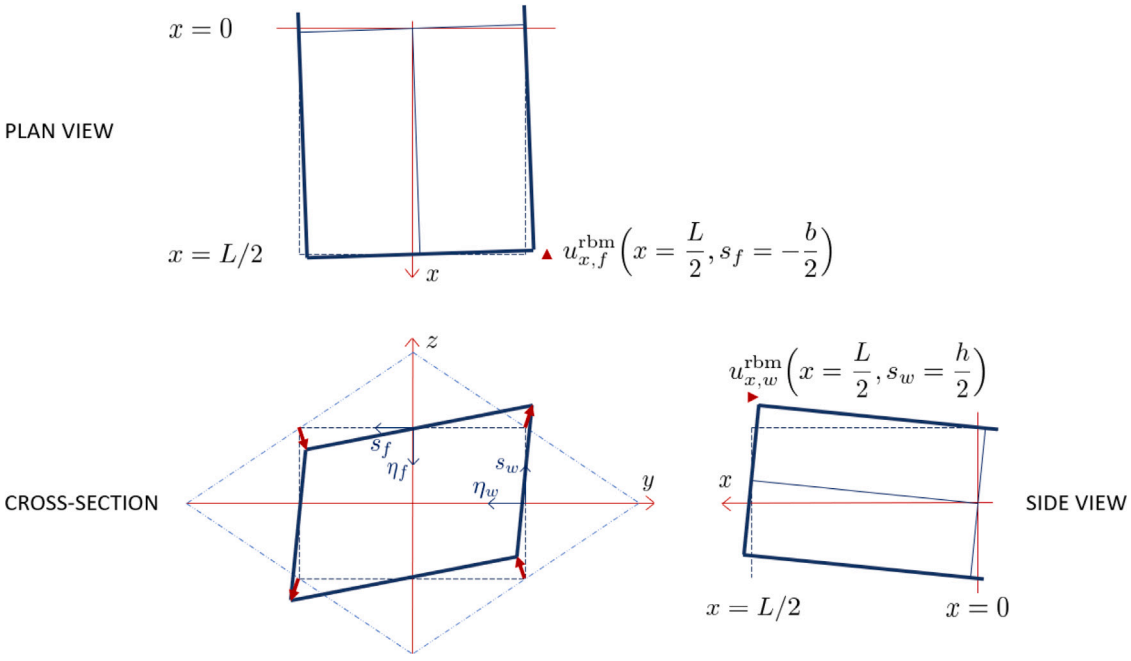

Fig. 5. Warping displacements at the upper-right corner of an end cross-section due to rigid body motions of the walls.

Now, the condition of vanishing resultant moment can be enforced:

$$2GJ_f\theta'_f + 2GJ_w\theta'_w + G\hat{J}\,\frac{1}{2}\left(1 - \frac{b}{D}\right)\gamma'_D = 0. \tag{18}$$

Plugging in the rates of rotation of the walls in terms of the rate of distortion (8) allows to solve for the parameter defining the position of the rotation centres, D:

$$D = \frac{\hat{J} + 2(J_f + J_w)}{\hat{J} + 4J_f}\, b. \tag{19}$$

As expected, if $J_f = J_w$ then $D = b$ and $M_x^{\mathrm{shear}} = 0$. On the other hand, if the torsion constant of the walls is much smaller than the torsion constant of the closed cross-section then $D \to b$ and $M_x^{\mathrm{shear}} \to 0$ as well. $D > b$ when $J_w > J_f$, and vice versa.

The numerator of the right-hand side of Eq. (19)

$$J = \hat{J} + 2(J_f + J_w) \tag{20}$$

is an approximation to the torsion constant of a rectangular box cross-section when the thickness of the walls is not neglected: while $\hat{J}$ only considers the constant shear flow along the walls, J also includes the effect of the circulation of shear stresses on each wall. Using (20), the value of D to match the condition of vanishing moment can be rewritten as:

$$D = \frac{J}{J + 2(J_f - J_w)}\, b. \tag{21}$$

Note that one is not bound to choose this canonical value of D. However, for an arbitrary choice of D, it is necessary to add an additional term to Eq. (18) to achieve zero torsional moment; this term is the torsional moment corresponding to a constant rotation rate θ'_x of the whole cross-section:

$$2GJ_f\theta'_f + 2GJ_w\theta'_w + G\hat{J}\,\beta\,\gamma'_D + G(\hat{J} + 2J_f + 2J_w)\theta'_x = 0, \tag{22}$$

where the following parameter has been introduced to improve readability:

$$\beta = \frac{1}{2}\left(1 - \frac{b}{D}\right). \tag{23}$$

Rearranging this expression and using Eq. (20) yields the condition of zero total torsional moment for an arbitrary value of D:

$$GJ\,\theta'_x + G(\beta J + J_f - J_w)\,\gamma'_D = 0. \tag{24}$$

This expression is analogue to the condition of zero axial force in a section subjected to simple bending where the origin is not located on the centroid:

$$EA\,u' + ES_y\,\theta'_y = 0. \tag{25}$$

This analogy brings to light the fact that the geometric interpretation of the total torsional rotation θ_x depends on the choice of D in the same way that the meaning of longitudinal displacement u of the centreline depends on the choice of origin for the cross section in (25). In contrast, the definition of the distortion angle γ_D is independent of D, as happens for the flexural rotation in the bending analogue. The term $(\beta J + J_f - J_w)$ plays the same role as the first moment of area: it vanishes for the principal value of D —Eq. (21)—.

3.2. Consistent definition of internal distortional moments

The internal distortional moment can be derived from the principle of virtual work. The internal virtual work is the sum of the work done by the twisting moment on each wall along the corresponding virtual twist $\delta\theta'_f$, $\delta\theta'_w$, and the work done by the shear flow $M_x^{\mathrm{shear}} = G\hat{J}\,\beta\,\gamma'_D$ along the virtual twist $\delta\theta'^{\,\mathrm{shear}}_x = M_x^{\mathrm{shear}}/G\hat{J} = \beta\,\gamma'_D$:

$$\begin{aligned}\delta W^{\mathrm{int}} &= \int_{-L/2}^{L/2} \left(2GJ_f\,\theta'_f\,\delta\theta'_f + 2GJ_w\,\theta'_w\,\delta\theta'_w + G\hat{J}\,\beta\,\gamma'_D\,\beta\,\delta\gamma'_D\right) \mathrm{d}x \\ &= \int_{-L/2}^{L/2} G\left(2(\beta + 1/2)^2 J_f + 2(\beta - 1/2)^2 J_w + \beta^2\hat{J}\right)\gamma'_D\,\delta\gamma'_D\,\mathrm{d}x.\end{aligned} \tag{26}$$

The quantity inside the big parenthesis defines the *distortion constant* J_D of the cross section. Selecting the principal value of D, (21), taking into account that $J = \hat{J} + 2(J_f + J_w)$ and rearranging, yields the distortion constant for rectangular box cross-sections

$$J_D^{pr} = \frac{1}{2}(J_f + J_w) - \frac{(J_f - J_w)^2}{J}, \tag{27}$$

that corresponds to the principal choice of centres of rotation. When $J_f = J_w$, J_D^{pr} is equal to the torsion constant of one wall. Note that this is precisely the value derived for the square box cross section —see the right-hand side of Eq. (2)—. As expected, the distortion constant is much lower than the torsion constant even for moderately thick walls.

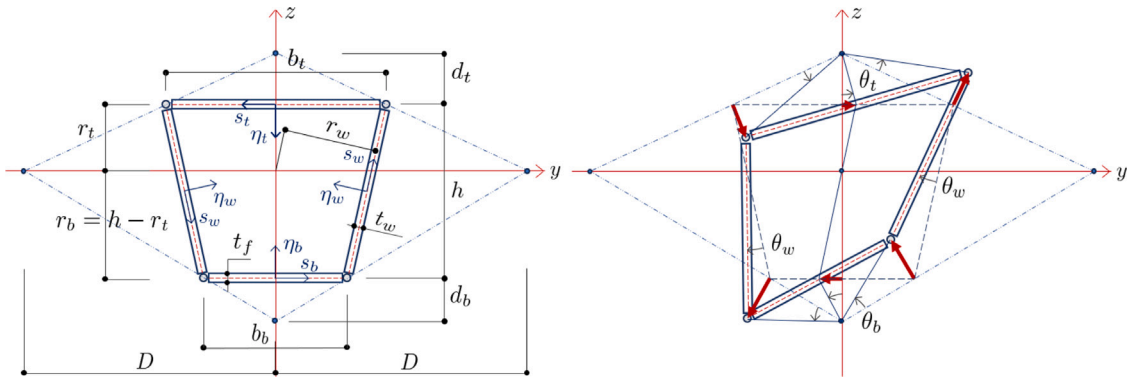

Fig. 6. General distortional pattern of a symmetric box girder cross section.

The internal virtual work can be expressed as

$$\delta W^{\text{int}} = \int_{-L/2}^{L/2} M_D \, \delta\gamma_D' \, \mathrm{d}x, \tag{28}$$

where the co-factor of the virtual distortional strain provides the *constitutive definition* of the internal distortional moment in terms of the distortion constant J_D^{pr}:

$$M_D = G J_D^{pr} \gamma_D'. \tag{29}$$

4. Torsional–distortional behaviour of symmetric trapezial box beams

In this section, we extend the previous results to a straight beam with symmetric trapezial section subjected to opposite sets of anti-symmetric forces applied at the end sections, and we show that in general, pure torsion and distortion are coupled.

The relevant dimensions of the cross section mid-line, the parameters defining the positions of the centres of rotation and an arbitrary distortional motion have been represented in Fig. 6. Subscripts t, b and w refer to the top flange, bottom flange and web, respectively. All results in this section are applicable to a trapezial box cross section in which the top flange has lateral cantilevers. In this case, in subsequent expressions, J_t would represent Bredt's torsion constant of the whole top flange, including the cantilevers. Nevertheless, the dimension b_t would remain the distance between the webs at the level of the top flange.

4.1. Kinematics

The basic kinematic assumptions are the same as for the rectangular section. The anti-symmetric distortional pattern is defined by four parameters (Fig. 6): d_t and d_b are the distances of the centres of rotation of the top and bottom flanges to the mid-lines of the flanges, r_t is the distance from the midline of the top flange to the line joining the centres of rotation of the web plates, r_w is the distance from the intersection of the lines joining opposite rotation centres to the midline of each web, and D is the distance of the centres of rotation of the web plates to the symmetry axis.

The description of the kinematics of the trapezial cross-section is more involved than the kinematics of the rectangular one. The geometric relations that link the rotations of the walls with the distortion of the cross-section are worked out in the Appendix. The distortion angle of a given section γ_D is defined as the average of the change in the angle of opposite corners of the cross-section. The change in each opposite corner is the sum of the rotations of the adjacent flange and web:

$$\gamma_D = \frac{1}{2}(\theta_t + \theta_b) - \theta_w. \tag{30}$$

According to the Appendix, Eq. (A.13), and Fig. 6, the wall rotations caused by the distortion are:

$$\theta_t = \alpha_t \alpha_b \Big(\Big(\frac{1}{\alpha_t} - \frac{1}{2} \Big) + \beta \Big) \gamma_D, \tag{31a}$$

$$\theta_w = -\alpha_t \alpha_b \Big(\frac{1}{2} - \beta \Big) \gamma_D, \tag{31b}$$

$$\theta_b = \alpha_t \alpha_b \Big(\Big(\frac{1}{\alpha_b} - \frac{1}{2} \Big) + \beta \Big) \gamma_D, \tag{31c}$$

with the following definitions for the geometric parameters:

$$\bar{b} = \frac{b_t + b_b}{2}, \qquad \alpha_t = \frac{b_t}{\bar{b}}, \qquad \alpha_b = \frac{b_b}{\bar{b}}, \qquad \beta = \frac{1}{2}\Big(1 - \frac{\bar{b}}{D}\Big). \tag{32}$$

With the previous considerations, the in-plane kinematics of the trapezial cross-section due to the torsional rotation $\theta_x(x)$ and the distortion $\gamma_D(x)$ is described by (cf. Eqs. (A.15)):

Top flange:
$$u_{s,t}(x) = r_t \Big(\theta_x - \alpha_t \alpha_b \Big(\frac{1}{2} - \beta \Big) \gamma_D \Big), \tag{33a}$$

$$u_{\eta,t}(x, s_t) = s_t \Big(\theta_x + \alpha_t \alpha_b \Big(\Big(\frac{1}{\alpha_t} - \frac{1}{2} \Big) + \beta \Big) \gamma_D \Big). \tag{33b}$$

Web:
$$u_{s,w}(x) = r_w \, \theta_x + \Big(\frac{h}{h_w} D - r_w \Big) \alpha_t \alpha_b \Big(\frac{1}{2} - \beta \Big) \gamma_D, \tag{33c}$$

$$u_{\eta,w}(x, s_w) = s_w \Big(\theta_x - \alpha_t \alpha_b \Big(\frac{1}{2} - \beta \Big) \gamma_D \Big). \tag{33d}$$

Bottom flange:
$$u_{s,b}(x) = r_b \Big(\theta_x - \alpha_t \alpha_b \Big(\frac{1}{2} - \beta \Big) \gamma_D \Big), \tag{33e}$$

$$u_{\eta,b}(x, s_b) = s_b \Big(\theta_x + \alpha_t \alpha_b \Big(\Big(\frac{1}{\alpha_b} - \frac{1}{2} \Big) + \beta \Big) \gamma_D \Big). \tag{33f}$$

4.2. Compatibility of warping displacements

Because of the anti-symmetry of the deformation of the cross-section, the u_x warping component of the midline displacement of both top and bottom flange midpoints must vanish. The u_x warping displacements of the midline are due to rigid body motions of the walls, as well as to their in-plane shear deformation. Therefore, the accumulated warping from the top to the bottom flange midpoints must vanish too. The following equations provide the warping increments due to rigid body motions of the walls caused by torsion and distortion; they have been evaluated starting from the midpoint of the top flange, advancing in the counter-clockwise direction, and ending at the midpoint of the bottom flange, following the same argument used in Fig. 5:

Top fl.:
$$\Delta u_{x,t}^{\text{rbm}} = -\frac{b_t}{2} r_t \, \theta_x' + \frac{b_t}{2} r_t \, \alpha_t \alpha_b \Big(\frac{1}{2} - \beta \Big) \gamma_D', \tag{34a}$$

Web:
$$\Delta u_{x,w}^{\text{rbm}} = -h_w r_w \, \theta_x' - h_w \Big(\frac{h}{h_w} D - r_w \Big) \alpha_t \alpha_b \Big(\frac{1}{2} - \beta \Big) \gamma_D', \tag{34b}$$

Bottom fl.:
$$\Delta u_{x,b}^{\text{rbm}} = -\frac{b_b}{2} r_b \, \theta_x' + \frac{b_b}{2} r_b \, \alpha_t \alpha_b \Big(\frac{1}{2} - \beta \Big) \gamma_D'. \tag{34c}$$

Adding the three contributions and taking into account that

$$\frac{1}{2}r_t b_t + \frac{1}{2}r_b b_b + r_w h_w = \bar{b}h \tag{35}$$

and the definition of β in Eq. (32), yields

$$\begin{aligned}\Delta u_x^{\text{rbm}} &= \Delta u_{x,t}^{\text{rbm}} + \Delta u_{x,w}^{\text{rbm}} + \Delta u_{x,b}^{\text{rbm}} \\ &= -\bar{b}h\,\theta'_x - (D-\bar{b})\,h\,\alpha_t\alpha_b\Big(\frac{1}{2}-\beta\Big)\gamma'_D \\ &= -\bar{b}h\,(\theta'_x + \alpha_t\alpha_b\,\beta\,\gamma'_D).\end{aligned} \tag{36}$$

A shear flow N_{xs} is needed to cancel the warping increment between top and bottom intersections of the midline with the symmetry axis. Assuming N_{xs} positive in the counter-clockwise direction, the warping increment due to the shear flow from top to bottom is:

$$\Delta u_x^{\text{shear}} = \frac{1}{2}\frac{N_{xs}}{G}\Big(\frac{b_t}{t_t} + \frac{2h_w}{t_w} + \frac{b_b}{t_b}\Big). \tag{37}$$

The magnitude of N_{xs} follows from the condition of zero net-warping,

$$\Delta u_x^{\text{rbm}} + \Delta u_x^{\text{shear}} = 0, \tag{38}$$

yielding:

$$N_{xs} = 2G\frac{\bar{b}h}{\frac{b_t}{t_t}+\frac{2h_w}{t_w}+\frac{b_b}{t_b}}(\theta'_x + \alpha_t\alpha_b\,\beta\,\gamma'_D) = \frac{1}{2\bar{b}h}G\hat{J}\,(\theta'_x + \alpha_t\alpha_b\,\beta\,\gamma'_D), \tag{39}$$

where $\hat{J}$ is Bredt's torsion constant. This shear flow is statically equivalent to

$$M_x^{\text{shear}} = 2\bar{b}hN_{xs} = G\hat{J}\,(\theta'_x + \alpha_t\alpha_b\,\beta\,\gamma'_D), \tag{40}$$

which is the fraction of the total torsional moment needed to enforce the compatibility of warping displacements at the corners of the cross-section. Note that the expression (17) deduced for the rectangular section is a particular case of (40) when there is no torsion.

4.3. Constitutive equations

The internal virtual work is the sum of the virtual work due to the rotation of each wall plus the virtual work done by the shear flow (40):

$$\begin{aligned}\delta W^{int} = \int_{-\frac{L}{2}}^{\frac{L}{2}}\Big(&GJ_t(\theta'_x+\theta'_t)(\delta\theta'_x+\delta\theta'_t) \\ &+2GJ_w(\theta'_x+\theta'_w)(\delta\theta'_x+\delta\theta'_w)+GJ_b(\theta'_x+\theta'_b)(\delta\theta'_x+\delta\theta'_b) \\ &+G\hat{J}(\theta'_x+\alpha_t\alpha_b\,\beta\,\gamma'_D)(\delta\theta'_x+\alpha_t\alpha_b\,\beta\,\delta\gamma'_D)\Big)\,\mathrm{d}x.\end{aligned} \tag{41}$$

Substituting the expressions of the wall rotation rates according to Eqs. (31), collecting the factors of the virtual strains $\delta\theta'_x$ and $\delta\gamma'_D$ and simplifying yields

$$\delta W^{int} = \int_{-\frac{L}{2}}^{\frac{L}{2}}\Big((C_{\theta\theta}\,\theta'_x + C_{\theta\gamma}\,\gamma'_D)\,\delta\theta'_x + (C_{\gamma\theta}\,\theta'_x + C_{\gamma\gamma}\,\gamma'_D)\,\delta\gamma'_D\Big)\,\mathrm{d}x. \tag{42}$$

with

$$C_{\theta\theta} = GJ, \tag{43a}$$

$$C_{\theta\gamma} = C_{\gamma\theta} = G\,\alpha_t\alpha_b\,(\beta J + J_{f-w}), \tag{43b}$$

$$C_{\gamma\gamma} = GJ_D, \tag{43c}$$

and

$$J = \hat{J} + J_t + 2J_w + J_b \tag{44a}$$

$$J_{f-w} = \Big(\frac{1}{\alpha_t}-\frac{1}{2}\Big)J_t + \Big(\frac{1}{\alpha_b}-\frac{1}{2}\Big)J_b - J_w, \tag{44b}$$

$$J_{f+w} = 2\Big(\frac{1}{\alpha_t}-\frac{1}{2}\Big)^2 J_t + 2\Big(\frac{1}{\alpha_b}-\frac{1}{2}\Big)^2 J_b + J_w, \tag{44c}$$

$$J_D = \alpha_t^2\alpha_b^2\Big(\beta^2 J + 2\beta J_{f-w} + \frac{1}{2}J_{f+w}\Big). \tag{44d}$$

The constitutive definition of the internal torsional and distortional moments follows from the cofactors of the virtual strains in (42):

$$\begin{bmatrix}M_x\\ M_D\end{bmatrix} = \begin{bmatrix}C_{\theta\theta} & C_{\theta\gamma}\\ C_{\gamma\theta} & C_{\gamma\gamma}\end{bmatrix}\begin{bmatrix}\theta'_x\\ \gamma'_D\end{bmatrix}. \tag{45}$$

With these definitions, the internal virtual work reads

$$\delta W^{int} = \int_{-\frac{L}{2}}^{\frac{L}{2}}\Big(M_x\,\delta\theta'_x + M_D\,\delta\gamma'_D\Big)\,\mathrm{d}x. \tag{46}$$

The constitutive equations are fully uncoupled when

$$\beta = \beta_{pr} = -\frac{J_{f-w}}{J} \Rightarrow D = D_{pr} = \frac{J}{J+2J_{f-w}}\bar{b}, \tag{47}$$

where D_{pr} defines the *principal centres of rotation* of the webs. In this case,

$$M_x = GJ\,\theta'_x, \qquad M_D = GJ_D^{pr}\,\gamma'_D, \tag{48}$$

with the distortion constant corresponding to the principal centres of rotation given by

$$J_D^{pr} = \alpha_t^2\alpha_b^2\Big(\frac{1}{2}J_{f+w} - \frac{J_{f-w}^2}{J}\Big). \tag{49}$$

4.4. External torsional and distortional moments

Let us first consider the action of anti-symmetrical forces F_y, F_z applied at the corners of the cross-section at $x = L/2$ and their opposites at $x = -L/2$ — Fig. 7, left—.

The external distortional moment, as well as the torsional moment, are consistently defined by means of the external virtual work as follows. According to the kinematic Eqs. (33), the virtual displacements in the s and η direction at the vertices are

$$\delta u_{s,t}|_{x=L/2} = r_t\Big(\delta\theta_x|_{\frac{L}{2}} - \alpha_t\alpha_b\Big(\frac{1}{2}-\beta\Big)\delta\gamma_D|_{\frac{L}{2}}\Big), \tag{50a}$$

$$\delta u_{\eta,t}|_{(x=L/2,s_t=\pm b_t/2)} = \pm\frac{b_t}{2}\Big(\delta\theta_x|_{\frac{L}{2}} + \alpha_t\alpha_b\Big(\Big(\frac{1}{\alpha_t}-\frac{1}{2}\Big)+\beta\Big)\delta\gamma_D|_{\frac{L}{2}}\Big), \tag{50b}$$

$$\delta u_{s,b}|_{x=L/2} = (h-r_t)\Big(\delta\theta_x|_{\frac{L}{2}} - \alpha_t\alpha_b\Big(\frac{1}{2}-\beta\Big)\delta\gamma_D|_{\frac{L}{2}}\Big), \tag{50c}$$

$$\delta u_{\eta,b}|_{(x=L/2,s_b=\pm b_b/2)} = \pm\frac{b_b}{2}\Big(\delta\theta_x|_{\frac{L}{2}} + \alpha_t\alpha_b\Big(\Big(\frac{1}{\alpha_b}-\frac{1}{2}\Big)+\beta\Big)\delta\gamma_D|_{\frac{L}{2}}\Big). \tag{50d}$$

The external virtual work of the point forces on the cross-section at $L/2$ is:

$$\begin{aligned}\delta W^{\text{ext}}|_{x=L/2} &= \pm 2F_z\,\delta u_{\eta,t}|_{(x=L/2,s_f=\pm b_t/2)} - 2F_y\,\delta u_{s,t}|_{x=L/2} \\ &\pm 2F_z\,\delta u_{\eta,b}|_{(x=L/2,s_f=\pm b_b/2)} - 2F_y\,\delta u_{s,b}|_{x=L/2} \\ &= 2\,(\bar{b}\,F_z - h\,F_y)\,\delta\theta_x|_{\frac{L}{2}} \\ &+ \big(\alpha_t\alpha_b\,(\bar{b}\,F_z + h\,F_y) + 2\,\alpha_t\alpha_b\,\beta\,(\bar{b}\,F_z - h\,F_y)\big)\,\delta\gamma_D|_{\frac{L}{2}}.\end{aligned} \tag{51}$$

Hence, the external torsional moment and distortional moment acting on the end section are the cofactors of the virtual rotation and the virtual distortion:

$$\widetilde{M}_x = 2\,(\bar{b}\,F_z - h\,F_y), \tag{52a}$$

$$\widetilde{M}_D = \alpha_t\alpha_b\,(\bar{b}\,F_z + h\,F_y) + 2\,\alpha_t\alpha_b\,\beta\,(\bar{b}\,F_z - h\,F_y). \tag{52b}$$

For the principal centres of rotation, the distortional moment is

$$\widetilde{M}_D^{pr} = \alpha_t\alpha_b\,(\bar{b}\,F_z + h\,F_y) - 2\,\alpha_t\alpha_b\,\frac{J_{f-w}}{J}\,(\bar{b}\,F_z - h\,F_y). \tag{53}$$

In sections with thin walls, $J_{f-w} \ll J$, and the second term can be neglected.

Ref. [8] includes a detailed derivation of the distortional moment caused by anti-symmetric vertical and horizontal forces causing torsional moments M_{xv} and M_{xh} respectively (Fig. 7, right). The derivation is based on the mentioned splitting of the loads into a torsional

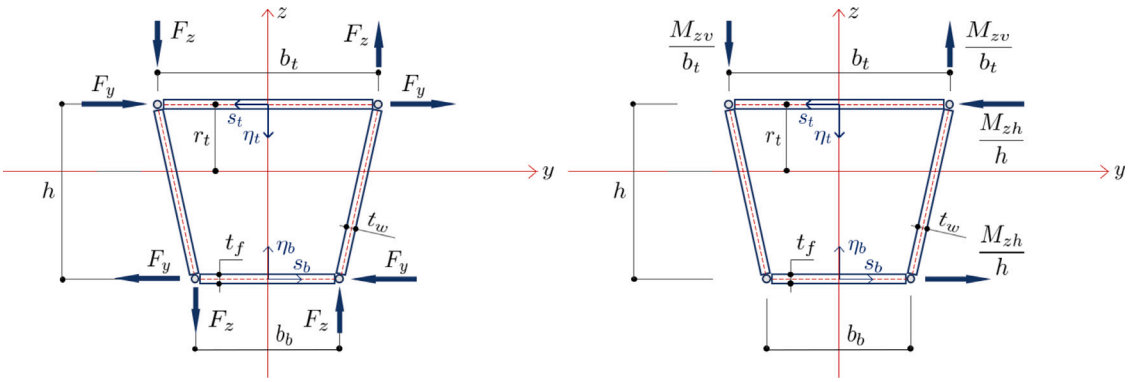

Fig. 7. Anti-symmetric force pattern on the end cross-section (left). Typical anti-symmetric loading, e.g. [8] (right).

part and a distortional part using equilibrium of a slice. Their result is (with our notation):

$$\widetilde{M}_D = \frac{1}{2}\left(M_{xv}\frac{b_b}{b_t} - M_{xh}\right) \tag{54}$$

Following the described procedure, our result is:

$$\widetilde{M}_D = \frac{1}{2}\alpha_t\alpha_b\left(M_{xv}\frac{b_b}{b_t} - M_{xh}\right) + \alpha_t\alpha_b\beta\left(M_{xv} + M_{xh}\right). \tag{55}$$

Choosing the principal centres of rotation, the second term is negligible. The first term is very similar to (54), except for the non-dimensional product $\alpha_t\alpha_b$ which is close to 1 for regularly sized cross-sections. The difference between the results is a consequence of our derivation being consistent with the principle of virtual work. The advantage of this approach based on the virtual work principle, is that it allows to calculate the consistent external distortional moments caused by *any* set of antisymmetric loads acting on the end sections.

4.5. Considerations about the distortional warping pattern

From Eqs. (34) and (37), the distortional warping pattern $\omega_D(s)$ is such that the warping displacements are $u_x = \omega_D(s)\,\gamma_D'$, and is composed of the following linear functions:

$$\text{Top fl.:} \quad \omega_{D,t}(s) = r_t\,\alpha_t\alpha_b\left(\frac{1}{2} - \beta\right)s + \frac{\hat{J}}{2\bar{b}\bar{h}}\,\alpha_t\alpha_b\,\beta\,s, \tag{56a}$$

$$\text{Bottom fl.:} \quad \omega_{D,b}(s) = (h - r_t)\,\alpha_t\alpha_b\left(\frac{1}{2} - \beta\right)s + \frac{\hat{J}}{2\bar{b}\bar{h}}\,\alpha_t\alpha_b\,\beta\,s. \tag{56b}$$

The warping pattern in the web is a linear function between the values at the top and bottom corners. The second term on the right hand side of Eqs. (56) is a consequence of the shear flow required for warping compatibility. The warping pattern depends on r_t, i.e., of the choice of the horizontal axis. However, it is remarkable that the shear flow required for compatibility, Eq. (39), and the constitutive equations, Eq. (45), are independent of r_t. This also applies to the distortional moment caused by anti-symmetric forces, Eqs. (53), which is independent of the position of the horizontal axis. Thus, the present theory is independent of the position of the horizontal axis. This is a similar situation as in Saint-Venant's torsion theory, that does not provide any information about the position of the rotation centre of the cross-section. Although in the previous developments we have chosen the same reference for describing torsion and distortion, the results remain valid when choosing different values of r_t for torsion and for distortion in Eqs. (34).

In cases with restrained warping (out of the scope of this paper), the distribution of normal stresses would be proportional to the warping pattern, and it would be necessary to choose a particular value for r_t in distortion, so that the moment of the pattern with respect to the horizontal axis is cancelled. This orthogonality requirement leads to the concept of *centre of distortion* that has been used in some references (e.g. [11,22]).

4.6. Validation

In this section we validate our model comparing the results with Finite Element models solved with the open-source code Kratos Multiphysics [23]. We have performed five numerical tests on 50 m long beams with hinged panels. Test cases have been labelled A to E. Cases A, B and C have the same thin-walled rectangular cross-section. Cases D and E correspond to trapezial cross-sections with thin and moderately thick walls respectively. The dimensions and relevant mechanical properties of each test case are included in Table 1; the distortion constant and the external distortional moment have been referred to the principal position of the rotation centres D_{pr}, reflected in the table, to work with uncoupled constitutive equations. Different sets of forces at the end cross-sections have been applied in each case: pure distortional forces in case A, pure torsional forces in case B, almost torsional forces in case C, and the same set of anti-symmetric forces in cases D and E. The details and the corresponding external torsional and distortional moments evaluated with Eq. (53) are included in Table 2.

In the FE model, the origin of the global reference system is placed at the central cross-section. The vertical axis is the symmetry axis of the cross-section and the section horizontal axis coincides with its shear centre. The rotation around the x-direction has been released in all nodes along the edges between web and flange panels to simulate the hinges. Translations along the 3 coordinate directions have been restrained at the nodes of the central cross-section where the warping component of the displacement should vanish according to the kinematics. Cross-section walls have been modelled with planar, transverse-shear-deformable 4-node quadrilateral shell elements with a maximum element size of $\Delta x = 1\,\text{m}$ in the x direction and $\Delta s = 0.5\,\text{m}$ along the cross-section midline. Each beam has been subjected to a set of anti-symmetric torsional–distortional forces at the corners of the end cross-sections ($x = -25\,\text{m}$ and $x = 25\,\text{m}$); the system of forces is completely defined by the values of the components $\mathbf{F}^{top,right} = [F_y, F_z]$ of the force applied at the top-right corner of the frontal $x = 25\,\text{m}$ cross-section. The FE model and the resulting deformation of Test A are represented in Fig. 8.

The results of the model and the FE simulation for the cross-section located at $x = L/4 = 12.5\,\text{m}$ are included in Table 3. To calculate the 1D model results for the torsional rotation and for the distortion we have first calculated the (constant) torsional and distortional rotation rates using the constitutive Eqs. (48), and then multiplied by the distance of the cross-section to the origin (12.5 m). Finally, the warping displacements follow from Eqs. (34). In the case of the FE models, the distortion is calculated evaluating the rotation of each wall from the coordinates of the corner nodes and then using Eq. (30); on the other hand the torsional rotation follows from subtracting the rotation of each wall caused by the distortion given by Eqs. (31) from the total rotation of the wall given by the corner coordinates, and averaging the results. Fig. 9 includes the representation of the forces, the in-plane

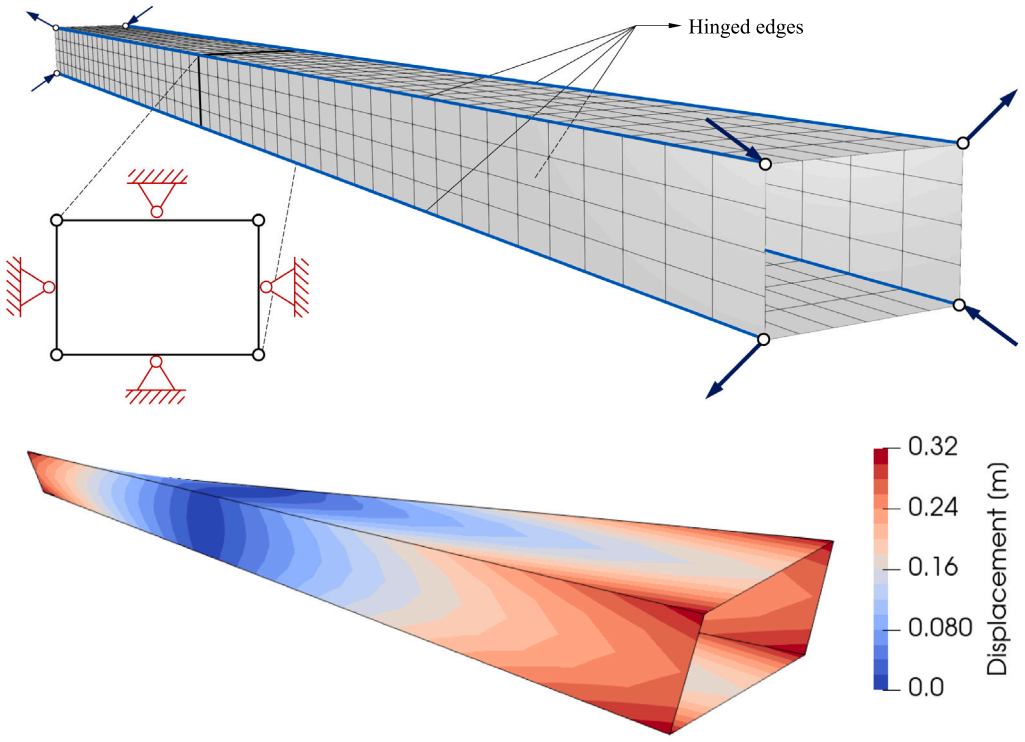

Fig. 8. Finite element model with boundary conditions and loads (top). Deformation (bottom). The model and the results correspond to test case A.

Table 1
Dimensions (m), position of the web rotation centres and mechanical properties of the various test cases.

Case	Shape	b_t	t_t	h	t_w	b_b	t_b	D_{pr} (m)	J (m^4)	J_D^{pr} (m^4)
A, B, C	rectangular	3.0	0.04	2.0	0.04	3.0	0.04	2.999 78	5.762×10^{-1}	5.333×10^{-5}
D	trapezial	5.0	0.05	2.0	0.025	3.0	0.05	3.998 36	7.558×10^{-1}	9.786×10^{-5}
E	trapezial	5.0	1.0	2.0	0.5	3.0	1.0	3.514 65	1.796×10^{1}	7.079×10^{-1}

Table 2
Applied forces and corresponding torsional and distortional moments.

Case	$\mathbf{F}^{\text{top,right}}$ (N)	Type of loading	M_x (N m)	M_D (N m)
A	[15 000.0, 10 000.0]	Pure distortional	0	6.000×10^{4}
B	[15 000.0, −10 001.481 043]	Pure torsional	-1.200×10^{5}	-1.038×10^{-6}
C	[15 000.0, −10 100.0]	Predominant torsion	-1.206×10^{5}	-2.995×10^{2}
D	[0, 10 000.0]	Mixed	8.000×10^{4}	3.748×10^{4}
E	[0, 10 000.0]	Mixed	8.000×10^{4}	3.232×10^{4}

Table 3
Torsional rotation, distortion and warping of the top-right corner of the section located at $x = L/4 = 12.5$ m for the different numerical tests.

Test		θ_x (rad)	γ_D (rad)	$u_x^{\text{top,right}}$ (m)
A	model	0	1.741×10^{-1}	-1.045×10^{-2}
	FEA	4.060×10^{-8}	1.740×10^{-1}	-1.047×10^{-2}
B	model	-3.223×10^{-5}	-3.012×10^{-12}	7.736×10^{-7}
	FEA	-3.222×10^{-5}	-7.580×10^{-7}	8.198×10^{-7}
C	model	-3.239×10^{-5}	-8.576×10^{-4}	5.223×10^{-5}
	FEA	-3.238×10^{-5}	-8.602×10^{-4}	5.238×10^{-5}
D	model	1.638×10^{-5}	5.928×10^{-2}	-5.399×10^{-3}
	FEA	1.486×10^{-5}	5.950×10^{-2}	-5.421×10^{-3}
E	model	6.893×10^{-7}	7.066×10^{-6}	-6.423×10^{-7}
	FEA	7.933×10^{-7}	8.412×10^{-6}	-7.647×10^{-7}

deformation and the warping displacements for every test. Note that the indicated scale of the deformation is different for each of tests and diagrams to provide a good visualisation of the difference between model and FEA results.

Case A corresponds to a thin-walled rectangular cross-section subjected to a pure distortional action. The model results show excellent agreement with the FE simulation.

Case B considers the same cross-section of the previous test subjected to a pure torsional action caused by anti-symmetric forces defined by their components [15 000, −10 001.481 043] N at the top-right corner. The decimal precision is required to cancel the distortional moment according to Eq. (53) —note that the distortional moment is 11 orders of magnitude smaller than the torsional moment (cf. Table 2).— The response is clearly torsional with negligible values for the distortion in both, our model and the FE simulation. The magnitude of the deformation is much smaller that in case A because the torsional stiffness is much higher than the distortional one (see Table 1.) It is remarkable to notice that the system of forces causing this pure torsional response is not orthogonal to the system causing pure distortion. An orthogonal system would produce the maximum value of the torsional moment for the given magnitude of the forces, but would also cause distortion, again according to Eq. (53).

The high sensitivity of the system to distortional deformations is illustrated by case C. In this test, anti-symmetric forces defined by

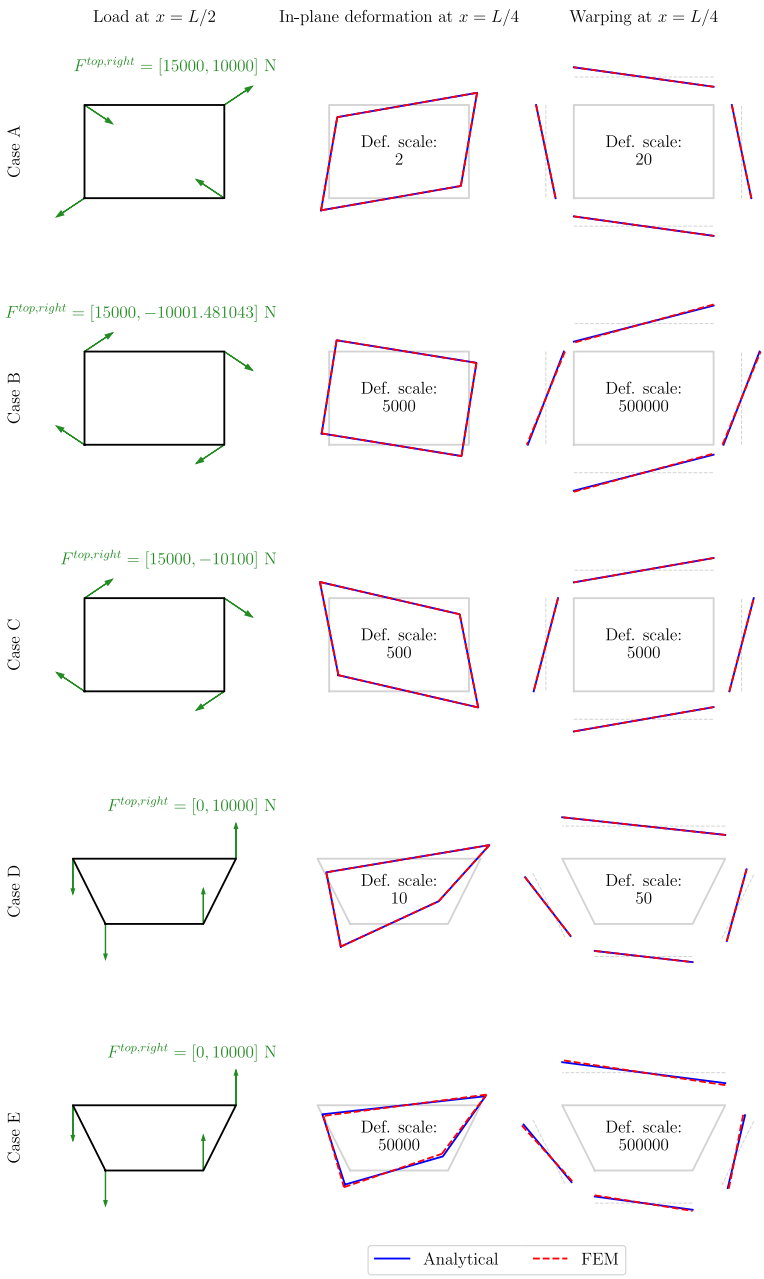

Fig. 9. Validation tests. End section loads and deformations at $x = L/4 = 12.5$ m.

[15 000, −10 100] N at the top-right corner have been applied. The horizontal component differs just 1 % from the one in Test B, however, the response is now dominated by the distortion in spite of the small difference. The match between our 1D model and the FE simulation is excellent.

In the last two test cases (D and E), anti-symmetric vertical forces of magnitude 10 000 N are applied to a beam with trapezial cross section. The cross-section of case D is thin-walled and the cross-section of case E has thicker walls. In case D, the relative difference between values of distortion and warping resulting from the 1D model and from FEA is lower than 0.4 %. However, the relative difference between values of the torsional rotation is higher (10.2 %), but the difference is not relevant considering the much lower order of magnitude of the torsional rotation, as demonstrated by the visual inspection of the deformation. The way in which the torsional rotation is estimated for the FE analyses justifies the mentioned percentage difference: as explained before, the torsional rotation follows from the estimated distortion; hence, a small error in the distortion is automatically amplified when the order of magnitude of the torsion is much lower than the order of the distortion. Finally, case E shows the behaviour when walls are thick. Since our model uses the thin-wall hypothesis, considerable errors were expected. The relative differences are higher (13.1 % for the torsional rotation, 16.0 % for the distortion and 9.8 % for the warping) but the 1D model can reproduce the overall deformation with reasonable accuracy.

5. Extension of the model for cross-sections with added distortional stiffness

It is straightforward to add to the internal virtual work (46) a term providing direct distortional stiffness resulting from the frame bending stiffness of the cross-section walls, ideally distributed stiffening frames or diagonal springs. Denoting the added stiffness by k_D, the virtual work equation $\delta W^{int} = \delta W^{ext}$ reads:

$$\int_0^L \left(\delta\theta_x' M_x + \delta\gamma_D' M_D + \delta\gamma_D\, k_D \gamma_D\right) \mathrm{d}x$$

$$= \widetilde{M}_x|_0\,\delta\theta_x|_0 + \widetilde{M}_D|_0\,\delta\gamma_D|_0 + \widetilde{M}_x|_L\,\delta\theta_x|_L + \widetilde{M}_D|_L\,\delta\gamma_D|_L, \tag{57}$$

where the tilde denotes the torsional and distortional moments applied at the start and end sections. (Note that the origin for the independent variable x is now at the start section.) Integration by parts provides the internal equilibrium equations,

$$M_x' = 0, \qquad M_D' - k_D\gamma_D = 0, \tag{58}$$

as well as the appropriate boundary terms. Substituting the constitutive Eqs. (45) into (58) yields the *equilibrium equations of pure torsion-distortion for a constant cross-section box beam* in terms of the generalised displacements:

$$C_{\theta\theta}\,\theta_x'' + C_{\theta\gamma}\,\gamma_D'' = 0, \tag{59a}$$

$$C_{\gamma\theta}\,\theta_x'' + C_{\gamma\gamma}\,\gamma_D'' - k_D\gamma_D = 0. \tag{59b}$$

The equations show that torsion and distortion are, in general, coupled.

It is possible to analyse problems with variable torsional and distortional moments using a similar approach as the one commonly used for closed or solid cross-sections subjected to torsion. For that purpose, the virtual work of the external distributed torsional and distortional loads,

$$\int_0^L \left(\delta\theta_x m_x + \delta\gamma_D m_D\right)\,\mathrm{d}x, \tag{60}$$

must be added to the right hand side of Eq. (57). Integrating by parts, the internal equilibrium equations become

$$M_x' + m_x = 0, \qquad M_D' - k_D\gamma_D + m_D = 0. \tag{61}$$

Choosing $D = D_{pr}$ uncouples the constitutive Eqs. (47); then,

$$M_x = GJ\,\theta_x', \qquad M_D = GJ_D^{pr}\,\gamma_D', \tag{62}$$

with the explicit expression of the distortion constant J_D^{pr} given by (49). In the following, we dispense with the superscript ^{pr} to avoid cluttered expressions. Substituting the constitutive equation into the equilibrium equation for the distortion yields

$$GJ_D\,\gamma_D'' - k_D\gamma_D + m_D = 0. \tag{63}$$

In the homogeneous case ($m_D = 0$), this equation coincides with Eq. (38) in Jönsson [18]. According to this author, the equation describes the "large scale" distortional behaviour of a closed thin-walled beam. This means that it provides a valid solution sufficiently far from cross-sections where distortion is constrained and warping gradients are strong, in spite of not having considered warping constraints nor in-plane bending of the cross-section walls.

The solution of the torsion equation in (61) is trivial and will not be discussed here. The general solution of the homogeneous distortion equation (63) ($m_D = 0$) is:

$$\begin{bmatrix}\gamma_D(\xi)\\ M_D(\xi)\end{bmatrix} = \begin{bmatrix}\cosh(\lambda\xi) & \frac{L}{GJ_D}\frac{\sinh(\lambda\xi)}{\lambda}\\ \frac{GJ_D}{L}\lambda\sinh(\lambda\xi) & \cosh(\lambda\xi)\end{bmatrix}\begin{bmatrix}\gamma_D(0)\\ M_D(0)\end{bmatrix}, \tag{64}$$

with the non-dimensional coordinate $\xi = x/L$, and the parameter

$$\lambda = L\sqrt{\frac{k_D}{GJ_D}}. \tag{65}$$

Finally, using (64), the solution for a simply supported beam (zero distortion at the end sections) subjected to a uniform external distributed distortional moment m_D is:

$$\gamma_D(\xi) = \frac{m_D L^2}{GJ_D}\,\frac{1}{\lambda^2}\left(\frac{\cosh(\lambda)-1}{\sinh(\lambda)}\sinh(\lambda\xi) - \cosh(\lambda\xi) + 1\right), \tag{66a}$$

$$M_D(\xi) = m_D L\,\frac{1}{\lambda}\left(\frac{\cosh(\lambda)-1}{\sinh(\lambda)}\cosh(\lambda\xi) - \sinh(\lambda\xi)\right). \tag{66b}$$

Fig. 10 represents the distortion given by Eq. (66a) in two different normalisations. On the left, it is normalised by the distortion constant: it is remarkable that for higher values of λ the distortion tends to be constant along the beam axis and its normalised value is very small, because J_D is very small. On the right, the distortion is normalised by the additional stiffness k_D; for higher values of lambda the normalised value equals 1 along most part of the domain, meaning that the distortion is simply given by the elastic relation $m_D = k_D\gamma_D$. This result is consistent with the fact that when λ has a large value, the distortion constant is negligible compared to the added distortional stiffness, and the distortional response is elastically determined by the stiffness of the section frame or by additional (distributed) diaphragms or springs.

A final comment on the external distributed moments: they must be calculated from the external distribution of surface forces. Starting from a general distribution, the first step is to extract the anti-symmetric part. Then, the density of external torsional moment m_x follows from a standard calculation. The consistent distributed distortional moment m_D is given by the external virtual work equation:

$$\int_0^L \delta\gamma_D\,m_D\,\mathrm{d}x = \int_0^L \left(2\int_{-h_{w,\inf}}^{h_{w,\sup}} \left(\delta u_{s,w}\,p_s + \delta u_{\eta,w}\,p_\eta\right)\,\mathrm{d}s_w + \int_{-b_t/2}^{b_t/2}\left(\delta u_{s,t}\,p_s + \delta u_{\eta,t}\,p_\eta\right)\,\mathrm{d}s_t + \int_{-b_b/2}^{b_b/2}\left(\delta u_{s,b}\,p_s + \delta u_{\eta,b}\,p_\eta\right)\,\mathrm{d}s_b\right)\mathrm{d}x, \tag{67}$$

where p_s, p_η are the components of the external surface forces acting on the cross-section walls referred to the adapted frame. The external distortional moment results from substituting the distortional part of the kinematic Eqs. (A.15) into the virtual displacements, factoring out $\delta\gamma_D$ and evaluating the integrals along the section mid-line inside the big parentheses.

We have shown in this section that the extended model produces estimates of the smoothed torsional rotations and distortional angles based on explicit expressions for the section parameters and the distributed distortional stiffness; the latter may include the bending stiffness of the section frame and the averaged distortional stiffness of intermediate diaphragms. Therefore, it is well suited to assess the global (or large-scale) torsional–distortional effects in long beams with closed cross-sections with moderately thick walls or with thin walls where the effect of internal stiffeners can be distributed along the length. However, the model cannot accurately estimate the stresses nor the gradients of the kinematic variables near sections where distortion is constrained. Further work is needed to determine the model's range of validity by quantifying the deviation between the extended model's results and those obtained with more sophisticated models.

6. Conclusions

In this paper, we present a one-dimensional model for the pure distortion and torsion of straight box beams with hinged walls and symmetric trapezial cross-section, in which the stiffness against distortional actions is solely provided by the torsional stiffness of each individual wall. Anti-symmetric loads are applied at the end cross-sections and no constraints to warping displacements are considered. In the last part of the paper, we propose an extended model to consider the distortional stiffness provided by the frame bending stiffness of the cross-section walls, as well as a consistent method to calculate distributed external distortional moments along the beam.

It can be concluded that:

1. The mathematical description of the pure torsional–distortional response of a box beam with symmetric cross-section is independent of the selected origin of coordinates on the symmetry axis (in analogy to Saint-Venant's torsion).
2. Our theory provides the relation between torsional and distortional moments, and torsional and distortional strains, in terms of a 2×2 constitutive matrix. Easy to evaluate, explicit expressions of the constitutive parameters have been derived. Torsion and distortion are generally coupled for an arbitrary position of the centres of rotation of the cross-section walls.

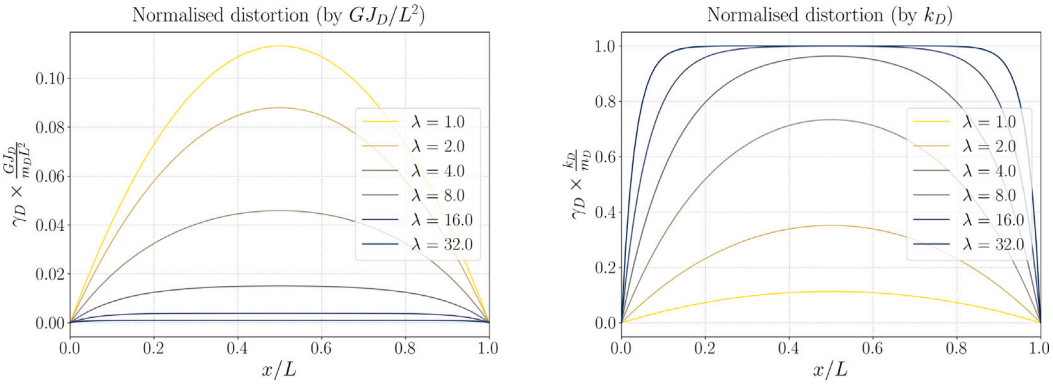

Fig. 10. Normalised distortion along the beam for different values of λ. Left: normalisation by the distortion constant. Right: normalisation by the additional distortional stiffness.

3. The distance of the centres of rotation of the web panels to the vertical symmetry axis influences the kinematic description and the definition of the parameters related to the distortion. There is one principal position of the rotation centres that uncouples the torsional and distortional response.
4. The principal position of the centres of rotation defines a principal distortion constant. As expected, the principal distortion constant is several orders of magnitude smaller than the torsion constant, except for sections with moderately thick walls.
5. The results of our model for beams with different proportions and wall thickness show very good agreement with the results of finite element models using shell elements.
6. We provide expressions for evaluating external distortional moments resulting from arbitrary anti-symmetric loads. The expressions are consistent with the principle of virtual work; hence, they are also applicable to more sophisticated distortion models.
7. The solution of the extended model (including distributed distortional stiffness) depends on the ratio between the additional distortional stiffness k_D and the intrinsic distortional rigidity GJ_D. The extended model is suitable to assess the large-scale torsional–distortional effects in long beams with closed cross sections with moderately thick walls or with thin walls where the effect of internal stiffeners can be distributed along the length.

Further work is needed to quantify the applicability of the extended model when the beam is subjected to non-constant distortional moments, and to adapt the model to composite cross-sections like the one motivating this research.

CRediT authorship contribution statement

Carlos Lázaro: Writing – review & editing, Writing – original draft, Validation, Methodology, Funding acquisition, Formal analysis, Conceptualization. **Guillermo Martínez-López:** Writing – review & editing, Visualization, Validation, Software, Methodology, Data curation, Conceptualization. **Kai-Uwe Bletzinger:** Writing – review & editing, Supervision, Project administration. **Roland Wüchner:** Writing – review & editing, Supervision, Methodology, Conceptualization.

Declaration of competing interest

The authors declare that they have no known competing financial interests or personal relationships that could have appeared to influence the work reported in this paper.

Data availability

Data will be made available on request.

Acknowledgements

This research was carried out during the stay of C. Lázaro at the Chair of Structural Analysis of the Technical University of Munich. This co-author gratefully acknowledges the support for his stay provided by the Universitat Politècnica de València and the retraining grant of the Spanish Ministry of Universities (RD 289/2021 and UNI/551/2021) funded by the European Union NextGenerationEU program. The authors thank also Salvador Monleón (UPV, Valencia) for the interesting discussions on this work.

Appendix. Kinematic relations in a symmetric trapezial cross-section

The parameters d_t, d_b, r_t and D defining the kinematics of cross-section are represented in Fig. 6. Only two of them are needed to describe the in-plane kinematics of the cross-section, because they are related by the following geometric relationships:

$$\frac{2\,d_t}{b_t} = \frac{d_t + r_t}{D}, \qquad \frac{2\,d_b}{b_b} = \frac{d_b + h - r_t}{D} = \frac{d_b + r_b}{D}. \tag{A.1}$$

It is convenient to select r_t, defining the position of the horizontal line joining the lateral centres, and D, distance of the lateral centres to the symmetry axis, as independent parameters. This is equivalent to selecting the location of the centres of rotation of the web plates. The location of the rotation centres of the flanges is then determined by the diagonal lines passing through the corners of the mid-line of the cross-section. Hence:

$$d_t = \frac{b_t}{2D - b_t} r_t, \qquad d_b = \frac{b_b}{2D - b_b} r_b. \tag{A.2}$$

The displacement vectors of the top and bottom left corners, considering only their in-plane components, can be expressed in horizontal and vertical coordinates in the plane of the cross-section as:

$$\mathbf{u}^{\text{top}} = \left[\, d_t\theta_t,\ -\frac{1}{2}b_t\theta_t \right]^{\mathsf{T}}, \qquad \mathbf{u}^{\text{bottom}} = \left[-d_b\theta_b,\ -\frac{1}{2}b_b\theta_b \right]^{\mathsf{T}}. \tag{A.3}$$

The unit vector from the top to the bottom left corners reads:

$$\boldsymbol{\lambda} = \left[\cos\phi,\ -\sin\phi \right]^{\mathsf{T}}, \tag{A.4}$$

where ϕ is the inner angle between the top flange and the web. The displacement of the points of the left web in the mid-line direction is constant along the web. Therefore,

$$u_{s,w} = \mathbf{u}^{\text{top}} \cdot \boldsymbol{\lambda} = \mathbf{u}^{\text{bottom}} \cdot \boldsymbol{\lambda}, \tag{A.5}$$

hence,

$$\left(d_t \cos\phi + \frac{1}{2} b_t \sin\phi \right) \theta_t = \left(-d_b \cos\phi + \frac{1}{2} b_b \sin\phi \right) \theta_b. \tag{A.6}$$

On the other hand, the following relations hold:

$$\cos\phi = \frac{b_t - b_b}{2h_w}, \qquad \sin\phi = \frac{h}{h_w}. \tag{A.7}$$

Substitution in the previous expression shows that the rotations of the top and bottom flanges are related as follows:

$$\left(b_t + (b_t - b_b)\frac{d_t}{h}\right)\theta_t = \left(b_b + (b_t - b_b)\frac{d_b}{h}\right)\theta_b. \tag{A.8}$$

The mid-line direction component of the displacement of the points of each flange is constant along it too. From this fact, it follows that the angle of rotation of both webs is the same regardless of their inclination, because it depends only on the difference between top and bottom flange displacements along the mid-line direction (constant along each flange) and on the vertical dimension of the cross-section h. This fact holds for the rotation of the segment located on the symmetry axis as well. Hence,

$$u_{s,t} = -d_t\,\theta_t = r_t\,\theta_w \qquad \Rightarrow \qquad \theta_t = -\frac{r_t}{d_t}\,\theta_w, \tag{A.9a}$$

$$u_{s,b} = -d_b\,\theta_b = (h - r_t)\,\theta_w \qquad \Rightarrow \qquad \theta_b = -\frac{h - r_t}{d_b}\,\theta_w = -\frac{r_b}{d_b}\,\theta_w. \tag{A.9b}$$

Now, we wish to express the rotation angles of each wall in terms of the distortion angle. Starting from the definition (7) of the distortion angle,

$$\gamma_D = \frac{1}{2}(\theta_t + \theta_b) - \theta_w, \tag{A.10}$$

and substituting the previous expressions of the angles yields

$$\gamma_D = -\frac{1}{2}\left(\frac{r_t}{d_t} + \frac{r_b}{d_b} + 2\right)\theta_w = -\frac{(b_t + b_b)}{b_t b_b}\,D\,\theta_w, \tag{A.11}$$

Using (A.2), (A.9) and (A.10), the rotation angles of the walls can be written in terms of the distortion as follows:

$$\theta_t = \left(\frac{2D - b_t}{b_t}\frac{b_t b_b}{(b_t + b_b)D}\right)\gamma_D(x) = \left(\frac{b_b}{\bar{b}} - \frac{b_t b_b}{\bar{b}^2}\frac{\bar{b}}{2D}\right)\gamma_D(x), \tag{A.12a}$$

$$\theta_w = -\frac{b_t b_b}{(b_t + b_b)D}\,\gamma_D(x) = -\frac{b_t b_b}{\bar{b}^2}\frac{\bar{b}}{2D}\,\gamma_D(x), \tag{A.12b}$$

$$\theta_b = \left(\frac{2D - b_b}{b_b}\frac{b_t b_b}{(b_t + b_b)D}\right)\gamma_D(x) = \left(\frac{b_t}{\bar{b}} - \frac{b_t b_b}{\bar{b}^2}\frac{\bar{b}}{2D}\right)\gamma_D(x), \tag{A.12c}$$

where $\bar{b} = (b_t + b_b)/2$ is the average width of the flanges. Note that the angles of rotation of the wall depend on D, but are independent of r_t. Finally, the wall rotations are expressed in terms of non-dimensional parameters for convenience:

$$\theta_t = \alpha_t\alpha_b\left(\left(\frac{1}{\alpha_t} - \frac{1}{2}\right) + \beta\right)\gamma_D, \tag{A.13a}$$

$$\theta_w = -\alpha_t\alpha_b\left(\frac{1}{2} - \beta\right)\gamma_D, \tag{A.13b}$$

$$\theta_b = \alpha_t\alpha_b\left(\left(\frac{1}{\alpha_b} - \frac{1}{2}\right) + \beta\right)\gamma_D, \tag{A.13c}$$

with the following definition for the non-dimensional parameters:

$$\alpha_t = \frac{b_t}{\bar{b}}, \qquad \alpha_b = \frac{b_b}{\bar{b}}, \qquad \beta = \frac{1}{2}\left(1 - \frac{\bar{b}}{D}\right). \tag{A.14}$$

Note that the definition of β is the similar to the one of the rectangular cross-section —Eq. (23).

Finally, taking into account Eqs. (A.9) and (A.13), the in-plane distortional kinematics of the trapezial cross-section is

Top fl.: $$u_{s,t}(x, s_t) = -d_t\theta_t = r_t\theta_w = -r_t\,\alpha_t\alpha_b\left(\frac{1}{2} - \beta\right)\gamma_D, \tag{A.15a}$$

$$u_{\eta,t}(x, s_t) = s_t\theta_t = s_t\,\alpha_t\alpha_b\left(\left(\frac{1}{\alpha_t} - \frac{1}{2}\right) + \beta\right)\gamma_D. \tag{A.15b}$$

Web: $$u_{s,w}(x, s_w) = -d_w\theta_w = \left(\frac{h}{h_w}D - r_w\right)\alpha_t\alpha_b\left(\frac{1}{2} - \beta\right)\gamma_D, \tag{A.15c}$$

$$u_{\eta,w}(x, s_w) = s_w\theta_w = -s_w\,\alpha_t\alpha_b\left(\frac{1}{2} - \beta\right)\gamma_D. \tag{A.15d}$$

Bottom fl.: $$u_{s,b}(x, s_b) = -d_b\theta_b = r_b\theta_w = -r_b\,\alpha_t\alpha_b\left(\frac{1}{2} - \beta\right)\gamma_D, \tag{A.15e}$$

$$u_{\eta,b}(x, s_b) = s_b\theta_b = s_b\,\alpha_t\alpha_b\left(\left(\frac{1}{\alpha_b} - \frac{1}{2}\right) + \beta\right)\gamma_D. \tag{A.15f}$$

References

[1] G. Martínez-López, C. Lázaro, R. Wüchner, K.-U. Bletzinger, Flutter mitigation in bridges by allowing the distortion of the deck, in: I. Calotescu, A. Chitez, C. Cosoiu, A.C. Vladut (Eds.), 8th European-African Conference on Wind Engineering - 8EACWE2022, 2022.

[2] V.Z. Vlassov, Piéces longues en voiles minces, second ed., Éditions Eyrolles, Paris, 1962, Trans. by G. Smirnoff.

[3] R.N. Wright, S.R. Abdel-Samad, A.R. Robinson, BEF analogy for analysis of box girders, J. Struct. Division ASCE 94 (7) (1968) 1719–1743, http://dx.doi.org/10.1061/JSDEAG.0002013.

[4] R. Dabrowski, Gekrümmte dünnwandige Träger: Theorie und Berechnung, Springer-Verlag, Berlin, Heidelberg, 1968, http://dx.doi.org/10.1007/978-3-642-50219-4.

[5] V. Křístek, Tapered box girders of deformable cross-section, J. Struct. Division ASCE 96 (8) (1970) 1761–1793, http://dx.doi.org/10.1061/JSDEAG.0002661.

[6] A. Steinle, Torsion und profilverformung beim einzelligen Kastenträger, Beton- und Stahlbetonbau 65 (9) (1970) 215–222.

[7] L. Boswell, S. Zhang, A box beam finite element for the elastic analysis of thin-walled structures, Thin-Walled Struct. 1 (4) (1983) 353–383, http://dx.doi.org/10.1016/0263-8231(83)90014-9.

[8] L. Boswell, S. Zhang, The effect of distortion in thin-walled box-spine beams, Int. J. Solids Struct. 20 (9) (1984) 845–862, http://dx.doi.org/10.1016/0020-7683(84)90054-4.

[9] L. Boswell, Q. Li, Consideration of the relationships between torsion, distortion and warping of thin-walled beams, Thin-Walled Struct. 21 (2) (1995) 147–161, http://dx.doi.org/10.1016/0263-8231(94)00030-4.

[10] Y.Y. Kim, J.H. Kim, Thin-walled closed box beam element for static and dynamic analysis, Internat. J. Numer. Methods Engrg. 45 (4) (1999) 473–490, http://dx.doi.org/10.1002/(SICI)1097-0207(19990610)45:4<473::AID-NME603>3.0.CO;2-B.

[11] N.-H. Park, S. Choi, Y.-J. Kang, Exact distortional behavior and practical distortional analysis of multicell box girders using an expanded method, Comput. Struct. 83 (19) (2005) 1607–1626, http://dx.doi.org/10.1016/j.compstruc.2005.01.003.

[12] C. Zhao, Y. Zhou, X. Zhong, G. Wang, Q. Yang, X. Hu, A beam-type element for analyzing the eccentric load effect of box girder bridges, Structures 36 (2022) 1–12, http://dx.doi.org/10.1016/j.istruc.2021.11.001.

[13] I. Campo-Rumoroso, Ó.-R. Ramos-Gutiérrez, F. Cambronero-Barrientos, Distortion analysis of horizontally curved trapezoidal box girder bridges, Eng. Struct. 282 (2023) 115798, http://dx.doi.org/10.1016/j.engstruct.2023.115798.

[14] R. Schardt, Verallgemeinerte technische Biegetheorie, Springer-Verlag, Berlin, Heidelberg, 1989.

[15] S.U. Benscoter, A theory of torsion bending for multicell beams, J. Appl. Mech. 21 (1) (1954) 25–34, http://dx.doi.org/10.1115/1.4010814.

[16] D. Camotim, N. Silvestre, R. Gonçalves, P.B. Dinis, GBT-based structural analysis of thin-walled members: overview, recent progress and future developments, in: M. Pandey, W.-C. Xie, L. Xu (Eds.), Advances in Engineering Structures, Mechanics & Construction, Springer, 2006, pp. 187–204.

[17] J. Jönsson, Distortional warping functions and shear distributions in thin-walled beams, Thin-Walled Struct. 33 (4) (1999) 245–268, http://dx.doi.org/10.1016/S0263-8231(98)00048-2.

[18] J. Jönsson, Distortional theory of thin-walled beams, Thin-Walled Struct. 33 (4) (1999) 269–303, http://dx.doi.org/10.1016/S0263-8231(98)00050-0.

[19] M.J. Andreassen, J. Jönsson, A distortional semi-discretized thin-walled beam element, Thin-Walled Struct. 62 (2013) 142–157, http://dx.doi.org/10.1016/j.tws.2012.07.011.

[20] F. Cambronero-Barrientos, J. Díaz-del-Valle, J.-A. Martínez-Martínez, Beam element for thin-walled beams with torsion, distortion, and shear lag, Eng. Struct. 143 (2017) 571–588, http://dx.doi.org/10.1016/j.engstruct.2017.04.020.

[21] R. Gonçalves, M. Ritto-Corrêa, D. Camotim, A new approach to the calculation of cross-section deformation modes in the framework of generalized beam theory, Comput. Mech. 46 (5) (2010) 759–781, http://dx.doi.org/10.1007/s00466-010-0512-2.

[22] M. Arici, M.F. Granata, Unified theory for analysis of curved thin-walled girders with open and closed cross section through HSA method, Eng. Struct. 113 (2016) 299–314, http://dx.doi.org/10.1016/j.engstruct.2016.01.051.

[23] V. Mataix, P. Bucher, R. Zorrilla, R. Rossi, J. Cotela, A. Cornejo, M.A. Celigueta, J.M. Carbonell, T. Teschemacher, C. Roig, M. Maso, G. Casas, S. Warnakulasuriya, M.N. nez, P. Dadvand, S. Latorre, I. de Pouplana, J. Irazábal, F. Arrufat, A. Ghantasala, K.B. Sautter, P. Wilson, B. Chandra, A. Geiser, I. López, et al., KratosMultiphysics/Kratos: release 9.4.2 (v9.4.2), 2023, https://zenodo.org/records/8422380.